Redox Biology 42 (2021) 101918

Contents lists available at ScienceDirect

Redox Biology

journal homepage: www.elsevier.com/locate/redox

Research Paper

Lack of the antioxidant enzyme methionine sulfoxide reductase A in mice impairs RPE phagocytosis and causes photoreceptor cone dysfunction

Francesca Mazzoni [a], Ying Dun [a], Jade A. Vargas [a], Emeline F. Nandrot [b], Silvia C. Finnemann [a,*]

[a] Center for Cancer, Genetic Diseases and Gene Regulation, Department of Biological Sciences, Fordham University, 441 East Fordham Road, Bronx, NY, 10458, USA
[b] Sorbonne Université, INSERM, CNRS, Institut de La Vision, 17 Rue Moreau, F-75012, Paris, France

ARTICLE INFO

Keywords:
MsrA
Oxidative stress
Phagocytosis
Photoreceptors
Retina
Retinal pigment epithelium

ABSTRACT

Methionine sulfoxide reductase A (MsrA) is a widely expressed antioxidant enzyme that counteracts oxidative protein damage and contributes to protein regulation by reversing oxidation of protein methionine residues. In retinal pigment epithelial (RPE) cells in culture, MsrA overexpression increases phagocytic capacity by supporting mitochondrial ATP production. Here, we show elevated retinal protein carbonylation indicative of oxidation, decreased RPE mitochondrial membrane potential, and attenuated RPE phagocytosis in *msra*$^{-/-}$ mice. Moreover, electroretinogram recordings reveal decreased light responses specifically of cone photoreceptors despite normal expression and localization of cone opsins. Impairment in *msra*$^{-/-}$ cone-driven responses is similar from 6 weeks to 13 months of age. These functional changes match dramatic decreases in lectin-labeled cone sheaths and reduction in cone arrestin in *msra*$^{-/-}$ mice. Strikingly, cone defects in light response and in lectin-labeled cone sheath are completely prevented by dark rearing. Together, our data show that *msra*$^{-/-}$ mice provide a novel small animal model of preventable cone-specific photoreceptor dysfunction that may have future utility in analysis of cone dystrophy disease mechanisms and testing therapeutic approaches aiming to alleviate cone defects.

1. Introduction

The retina and neighboring retinal pigment epithelium (RPE) experience significant levels of chronic oxidative stress due to light exposure inherent to their location and function [1]. The resulting oxidative damage contributes to retinal aging and retinal diseases such as age-related macular degeneration, a common disease in the developed world that is characterized by impaired high acuity central vision due to the high density of cone photoreceptors in the macula.

Methionine residues are exquisitely sensitive to oxidation leading to a modification or loss of protein function when oxidized within proteins [2]. Sulfoxide reductase enzymes work in tandem with thioredoxin/thioredoxin reductases to reverse methionine oxidation. Methionine sulfoxide reductase A (MsrA) is a ubiquitous antioxidant enzyme -although its levels and subcellular localization differ among tissues-that functions in reducing specifically the S-diastereomer of methionine sulfoxide in free and protein bound methionines [3–6].

MsrA has high expression in the RPE *in vivo,* and its protective role for RPE cells culture has been well documented [7–9]. In addition to antioxidant defense, mitochondrial MsrA supports RPE ATP synthesis. In consequence, levels of MsrA directly correlate with capacity of RPE cells in culture to phagocytose photoreceptor outer segment fragments (POS), a characteristic and highly energy demanding function of RPE cells [10].

Global and constitutive targeted inactivation of the *msra* gene yields *msra*$^{-/-}$ mice that are viable and fertile but demonstrate moderate neurological abnormalities with characteristic features of neurodegenerative diseases [11]. In the eye, lack of MsrA causes lens abnormalities due to oxidative protein modifications [12]. Here, we explore *msra*$^{-/-}$ mice to identify the effects of constitutive lack of MsrA on RPE and neural retina phenotype and function *in vivo*.

We found elevated protein carbonylation indicative of oxidative damage and reduced mitochondrial activity in the RPE in eyes of young adult *msra*$^{-/-}$ mice in agreement with earlier studies [13,14]. Our results further confirm the key role of MsrA in RPE functionality as *msra*$^{-/-}$ RPE phagocytosis is attenuated in early adulthood compared to phagocytosis in age-matched wt mice. Dramatically reduced retinal light responses specifically of cone photoreceptors and of cone extracellular matrix even in young adulthood implies that MsrA activity is essential

Abbreviations: Electroretinogram, ERG; MsrA, methionine sulfoxide reductase A; POS, photoreceptor outer segment fragments; RPE, retinal pigment epithelium.

* Corresponding author. Department of Biological Sciences, Larkin Hall, Fordham University, 441 East Fordham Road, Bronx, NY, 10458, USA.
E-mail address: finnemann@fordham.edu (S.C. Finnemann).

https://doi.org/10.1016/j.redox.2021.101918
Received 8 December 2020; Received in revised form 2 February 2021; Accepted 20 February 2021
Available online 26 February 2021

for cone functionality and not compensated for in *msra*$^{-/-}$ mice. MsrA cone dysfunction did not worsen with age indicating that effects of loss of MsrA are not cumulative over time. Finally, dark rearing demonstrated that cone photoreceptor dysfunction due to lack of MsrA is fully preventable. Altogether *msra*$^{-/-}$ mice provide an exciting new experimental model for cone photoreceptor dysfunction.

2. Materials and methods

2.1. Reagents

Reagents were from Millipore-Sigma (St. Louis, MO) or Thermofisher (Carlsbad, CA) unless indicated.

2.2. Mice

Methionine Sulfoxide Reductase A knockout (*msra*$^{-/-}$) mice were studied previously [11]. Mice were routinely backcrossed to 129 T2/SvEmsJ wild-type (wt) mice, which served as control. All procedures were approved by the Institutional Animal Care and Use Committee of Fordham University (B08-02R). Experiments used mixed cohorts of female and male mice. Photoreceptor outer segment fragment (POS) phagocytosis does not vary with sex in mice [15]. Mice were housed in a 12-h light/12-h dark cycle and were provided water and standard chow ad libitum. For dark-rearing experiments, mice were bred and raised in darkness with handling under dim red light every morning. Mice were sacrificed at defined ages and times of day by CO_2 asphyxiation followed by immediate eye enucleation, tissue dissection and fixation for 30 min in 4% paraformaldehyde in PBS followed by standard cryopreservation in OCT or paraffin, sectioning, and processing for microscopy evaluation as appropriate. For protein biochemistry, dissected tissues were immediately snap frozen and stored at −80 °C prior to homogenization and analyses.

2.3. Quantification of protein carbonylation and ATP content

Frozen single whole eyeballs without cornea and lens, dissected neural retina or remaining posterior eyecups without neural retina were immersed in ice cold PBS and homogenized in an ice bath by applying a Tissue-Tearor (Biospec Products, Bartlesville, OK) 5 times for 5 s at 20,000 rpm. Following 1 min spin at 1000×*g* the supernatant was used immediately at 1:10 dilution in PBS in a Protein Carbonyl ELISA kit (Cell Biolabs, San Diego, CA) according to the manufacturer's instructions or in serial dilutions in the ENLITEN® ATP assay system (Promega, Madison, WI) according to the manufacturer's instructions. Each sample was adjusted for protein content and measured in duplicate. Wt and *msra*$^{-/-}$ tissues were directly compared in each assay. Positive and negative controls provided by the kits were included in each assay.

2.4. Live imaging of RPE mitochondria

Freshly dissected posterior eyecups without neural retina from one wt and one *msra*$^{-/-}$ mouse were incubated for 10 min at 37 °C with mitochondrial membrane potential-dependent MitoTracker™ Red CMXRos (Thermofisher #M7512) at 1 μM in Fluorobrite DMEM. Samples were flat mounted RPE side up in the same solution on glass slides and immediately imaged with a TSP8 Leica confocal system (Leica Microsystems, Wetzlar, Germany). The experiment was performed 4 times independently with identical acquisition parameters for all samples; all conducted 4–5 h after light onset. ImageJ was used to quantify area fluorescence intensity in maximal projections of z-stacks of equal thickness.

2.5. Protein extraction and immunoblotting

Individual whole eyeballs without cornea and lens, single dissected neural retinas or remaining posterior eyecups without neural retina were mechanically disrupted by pipetting in HNTG buffer (50 mM HEPES, 150 mM NaCl, 1% Triton-X100, 10% glycerol, pH 7.5) freshly supplemented with protease inhibitor cocktail followed by vortexing for 15 min. Equal volumes of cleared eyeball fractions were analyzed by standard SDS-PAGE and immunoblotting followed by enhanced chemiluminescence digital detection by a KwikQuant Imager (Kindle Biosciences, Greenwich, CT). Primary antibodies used are listed in Supplemental Table S1. Reprobing with α-tubulin-HRP was used for sample normalization. ImageJ was used to directly compare band intensities on individual blot membranes.

2.6. Whole-mount RPE preparation, labeling, and in situ phagosome quantification

Rod and cone outer segment fragment phagosome quantification *in situ* was described in detail previously [16–18]. Posterior eyecup whole mount preparations were stained with rhodopsin monoclonal antibody and a mix of S-cone opsin and L/M-cone opsin polyclonal antibodies (same antibodies as for immunoblotting, Supplemental Table S1) and AlexaFluor-conjugated secondary antibodies. Maximal projections of z-stacks of equal thickness acquired on a Leica TSP5 confocal system were used to separately quantify rod and cone phagosomes of 0.5 μm diameter and above using ImageJ.

2.7. Tissue sectioning, histological and immunofluorescence staining, TUNEL assay and microscopy analyses

Standard H&E was performed on deparaffinated tissue sections. For fluorescence microscopy, 14 μm thick cryosections were labeled with antibodies (Supplemental Table S1) or FITC-conjugated peanut agglutinin (PNA) and DAPI to counterstain nuclei. The ApopTag kit (Millipore-Sigma) was used for TUNEL staining of apoptotic nuclei. As positive control a retina section of a 35-day-old RCS rat with active retinal degeneration was also stained. Vectashield (Vector Laboratories; Burlingame, CA) mounted samples were imaged on a Leica TSP5 laser scanning confocal microscopy system. Quantification of fluorescence signal intensity over area were performed on maximal projections of 5 μm image stacks using ImageJ.

2.8. Electroretinography (ERG)

ERGs were recorded from dark adapted anesthetized mice exactly as described previously [19,20] using a UTAS-E2000 system (LKC Technologies, Gaithersburg, MD). Stimuli were presented in order of increasing intensity as series of white flashes of 1.5 cd-s/m^2 attenuated with neutral density filters to yield intensities from −1.8 to 0.2 log cd-s/m^2. Photopic ERGs were recorded after 5 min exposure to 20 cd/m^2 white background using an unattenuated white flash stimulus of 2.5 log cd-s/m^2. Six responses were recorded and averaged for each condition from each mouse followed by amplitude measurements.

2.9. Statistical analyses

All experiments were conducted at least three times and analyzed at least three independent biological samples. Data were analyzed using GraphPad Prism 8 (La Jolla, CA). ANOVA and post hoc tests or unpaired, two-tailed Student's t-test were used to determine differences between groups. P values < 0.05 were considered statistically significant.

3. Results

3.1. *msra*$^{-/-}$ mouse tissues show elevated levels of protein oxidation in the eye, reduced RPE mitochondrial activity, and impaired RPE phagocytosis

Introduction of carbonyl groups to side chains is the most common protein modification in tissues undergoing oxidative stress [13,14]. We previously correlated protein carbonylation with retinal dysfunction in mice [19]. Reduced levels of MsrA have been associated with increased protein carbonylation with age and cellular senescence [21–24]. *msra*$^{-/-}$ mice exhibit increased levels of protein carbonylation in kidney tissue under normal vivarium conditions and increase protein carbonylation in other tissues significantly more than wt mice within 24–48 h in response to hyperoxia [11]. To test whether loss of MsrA affects the retina/RPE under normal environmental conditions, we compared levels of protein carbonyl adducts in whole eye samples without lens, isolated neural retina, and posterior eyecups containing RPE and choroid of 10-week old wt and *msra*$^{-/-}$ mice [25,26]. We found a significant increase of carbonyl adducts in *msra*$^{-/-}$ whole eye tissues, by 78%, compared to wt eyes (Fig. 1A, bars whole eye). A trend towards elevated protein carbonylation was also seen in isolated neural retina and more so in RPE-choroid fractions but these differences to wt did not reach statistical significance (Fig. 1A, bars retina, eyecup).

To follow up on our previous finding that MsrA in RPE cells in culture supports mitochondrial ATP synthesis [27] we next imaged live freshly dissected RPE tissue stained with MitoTracker® Red CMX-Ros, a biosensor that fluoresces only in mitochondria with active membrane potential. In *ex vivo* experiments testing wt and *msra*$^{-/-}$ RPE side by side, the average intensity of *msra*$^{-/-}$ RPE mitochondria staining was only 44% of the staining intensity of wt RPE suggesting reduced mitochondrial function in *msra*$^{-/-}$ RPE *in vivo* (Fig. 1B and C). However, levels of mitochondrial proteins including those representing different protein complexes of the respiratory chain did not reveal significant

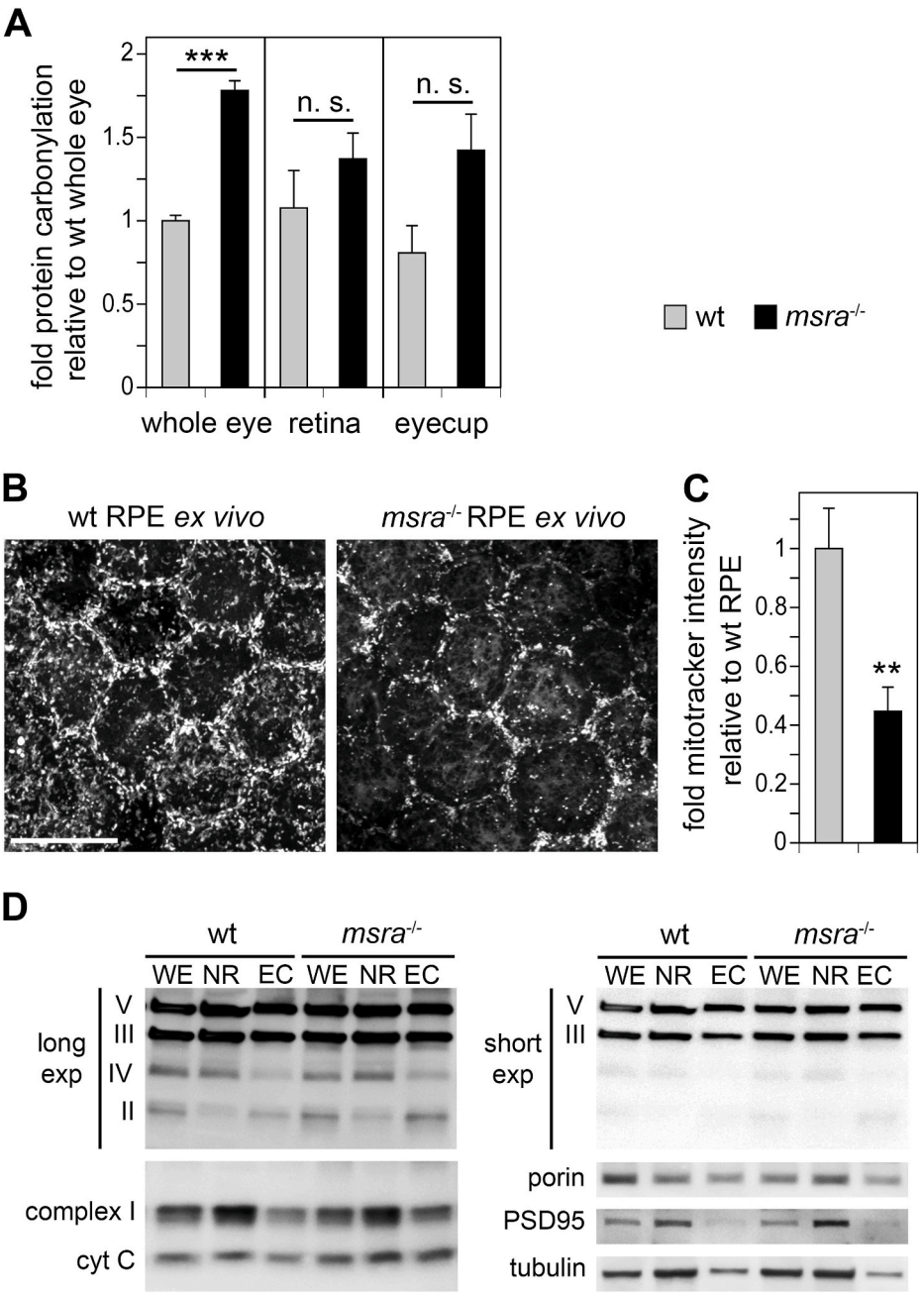

Fig. 1. *msra*$^{-/-}$ eyes show elevated protein carbonylation and reduced RPE mitochondrial activity but normal mitochondrial protein levels. (**A**) ELISA quantification of protein carbonylation in homogenates of whole eyes without lens (whole eye), dissected neural retina (retina) and posterior eyecups without retina (eyecup) fractions obtained from 10-week old wt and *msra*$^{-/-}$ mice. Bars show protein modification levels relative to levels of samples from wt whole eyes, which was set as 1; mean ± s.e.m., n = 4 samples from individual mice for whole eyes, and n = 3 for retina and eyecups. 2-way ANOVA statistical analysis per each condition revealed significant differences between whole eye samples as indicated; ***$p < 0.001$. (**B**) Representative live imaging fields of RPE in flat-mount eyecup tissue from 6 to 7 week-old wt and *msra*$^{-/-}$ mice live labeled with MitoTracker® Red CMXros. Images show maximal projections. (**C**) Intensity quantification of images as in (**B**). Bars show mean ± s.e.m., n = 4 mice per genotype. **$p < 0.01$. (**D**) Immunoblotting detection of mitochondrial and tissue marker proteins as indicated in whole eyes without lens (WE), dissected neural retina (NR) and posterior eyecups without retina (EC) fractions obtained from 6-7-week old wt and *msra*$^{-/-}$ mice. For detection of mitochondrial respiratory chain complexes, a mix of monoclonal antibodies was used that yielded specific bands for complexes II, III, IV, and V as indicated (panel long exp). For complexes III and V, a short exposure of the same blot membrane is shown in addition to illustrate equal level of these proteins without saturation issues (panel short exp). In addition, mitochondrial complex I marker protein, porin, cytochrome C (cyt C), neural retina marker PSD95, and total protein loading control α-tubulin were tested in panels as indicated. No bar graph quantification is shown as densitometry did not reveal any significant protein level differences after comparing tissues from 3 wt and 3 *msra*$^{-/-}$ mice each. Blots shown represent tissue fractions of 1 representative wt and *msra*$^{-/-}$ mouse, respectively.

differences between *msra*$^{-/-}$ and wt whole eyes, isolated neural retina or RPE/choroid (Fig. 1D). RPE cells *in vivo* are known to be capable of maintaining normal ATP levels through glycolysis even if mitochondrial respiration is abrogated [28]. Here, we directly compared ATP content in posterior eyecup tissue enriched in RPE/choroid from 6 week-old wt and *msra*$^{-/-}$ mice. A small decrease in ATP content in *msra*$^{-/-}$ tissue did not reach statistical significance (Supplemental Fig. S1). These results suggest that *msra*$^{-/-}$ RPE maintains normal ATP availability.

In RPE cells in culture, acute silencing of MsrA reduces POS phagocytosis [10]. Thus, we counted rod and cone POS phagosomes internalized by wt and *msra*$^{-/-}$ RPE *in situ*. We reasoned that any abnormality may be especially obvious at the time of greatest activity, the diurnal peak of RPE phagocytosis. Therefore, we chose to analyze tissues harvested 1.5 h after light onset, which is a time of maximal diurnal phagosome load [29]. Microscopy panels in Fig. 2 show flat mounted RPE co-stained with rhodopsin and cone opsin antibodies to identify rod and cone phagosomes in the same sample, respectively. Both rod and cone phagosomes appeared attenuated in *msra*$^{-/-}$ tissue (Fig. 2A,C). Phagosome quantification revealed that in 10-week old mice, rod phagosome content of *msra*$^{-/-}$ RPE decreased by 27% on average (Fig. 2B) while average cone phagosome content was reduced more severely, by 58% (Fig. 2D). Comparative quantitative immunoblotting of opsins and retinal markers demonstrated that the differences in opsin labeling of phagosomes were not caused by differences in levels of rhodopsin, S- or L/M-opsins, which were identical in wt and *msra*$^{-/-}$ eyes (Fig. 2E). These results demonstrate that lack of MsrA *in vivo* reduces RPE phagocytosis at the diurnal peak especially of cone POS.

3.2. Lack of MsrA specifically reduces cone photoreceptor matrix sheath and light responses

Next, we tested if lack of MsrA affects retinal morphology and photoreceptor function. Retinal section tissue histology showed normal appearance and organization of *msra*$^{-/-}$ retina in 6-week old mice (Fig. 3A). However, we observed a dramatic reduction in peanut agglutinin (PNA) stained interphotoreceptor matrix known to ensheath specifically cone photoreceptors (Fig. 3B). The outer nuclei layer (ONL) thickness of the central retina -commonly used to gauge photoreceptor cell numbers-was measured by counting numbers of photoreceptor nuclei across the ONL in tissue sections as shown in Fig. 3A. This quantification showed that ONL thickness of wt and *msra*$^{-/-}$ retina was identical (Fig. 3C). In contrast, quantification of cone sheath fluorescence signal revealed an 82% reduction in *msra*$^{-/-}$ retina on average (Fig. 3D).

To directly test retinal function, we next recorded electroretinograms of age-matched cohorts of wt and *msra*$^{-/-}$ mice. Scotopic ERGs -testing mainly rod responses with some contribution of cones at high light flash intensities-showed normal a-wave amplitudes in 6-week-old *msra*$^{-/-}$ mice implying fully functional rod light responses (Fig. 4A and B, panel a-wave). Scotopic b-wave amplitudes were moderately lower, by 20–35% on average, in *msra*$^{-/-}$ mice than in wt mice (Fig. 4A and B, panel b-wave). Photopic ERGs -testing cone photoreceptor activities alone-revealed robustly decreased cone activity by 49% on average in 6 week-old *msra*$^{-/-}$ mice (Fig. 4C and D, bars 6 weeks). Photopic ERG assessment of 6-month old and of 13 month-old *msra*$^{-/-}$ mice also showed large decreases in cone light responses (Fig. 4D, bars 6 months and 13 months). Moreover, direct comparison showed that the extent of the decrease compared to wt at the same age did not significantly vary across all 3 ages tested implying that cone dysfunction in *msra*$^{-/-}$ mice is not progressive (Fig. 4E).

To complete our phenotype assessment we performed comparative immunofluorescence microscopy showing close-up views to allow assessment of cell morphology and immunoblotting to allow quantification of well-established marker proteins for retinal neurons. We did not find significant differences between 6 week-old wt and *msra*$^{-/-}$ retina in distribution or steady-state protein level of rhodopsin (Fig. 5A,

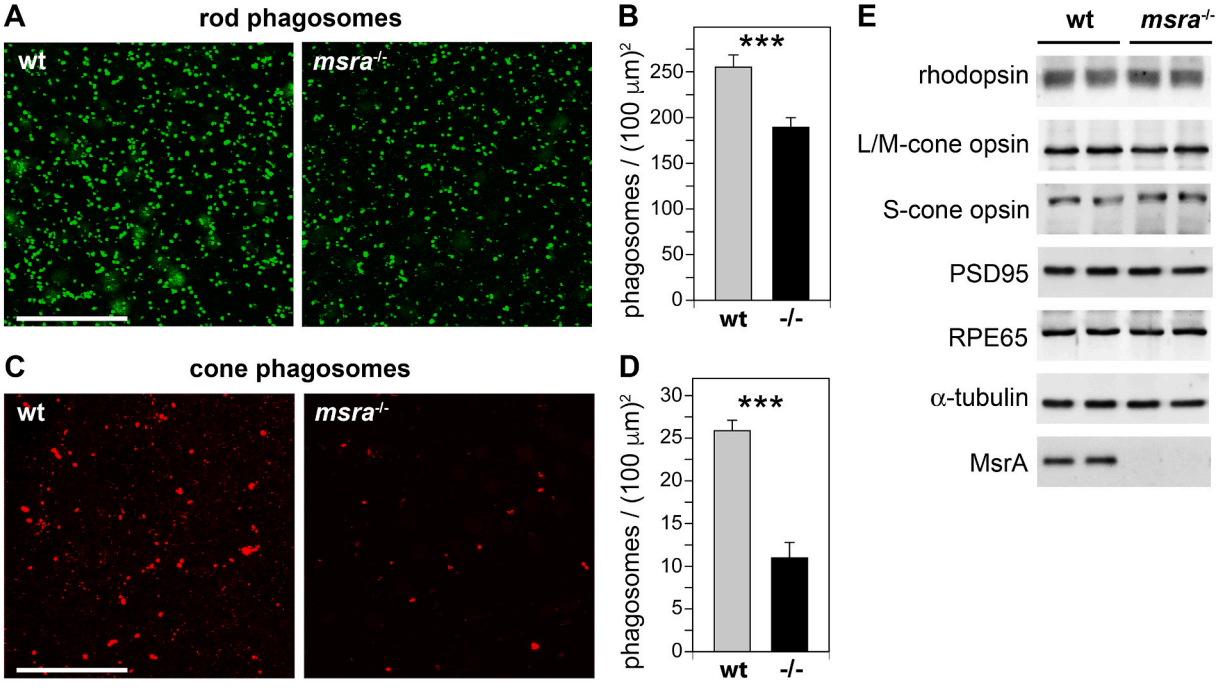

Fig. 2. Rod and cone phagosome content is decreased in *msra*$^{-/-}$ RPE after light onset. (**A,C**) Representative images of rod (green, **A**) and cone (red, **C**) phagosomes in RPE in flat-mount eyecup tissue obtained 1.5 h after light onset from 10-week old wt and *msra*$^{-/-}$ mice as indicated. Scale bars, 50 µm. Bars in **B** and **D** show quantification of rod and cone phagosome density, respectively, obtained from experiments as in **A** and **C** as mean ± s.e.m.; n = 5 eyes from 5 mice per sample. 2-way ANOVA with Tukey's multiple comparison revealed significant differences shown as $^{**}p < 0.01$ and $^{***}p < 0.001$. (**E**) Representative immunoblots showing equal marker protein content (probes as indicated) in whole eye extracts from 2 eyes from 2 different wt or *msra*$^{-/-}$ mice. No bar graph quantification is shown as densitometry did not reveal any protein level differences. (For interpretation of the references to colour in this figure legend, the reader is referred to the Web version of this article.)

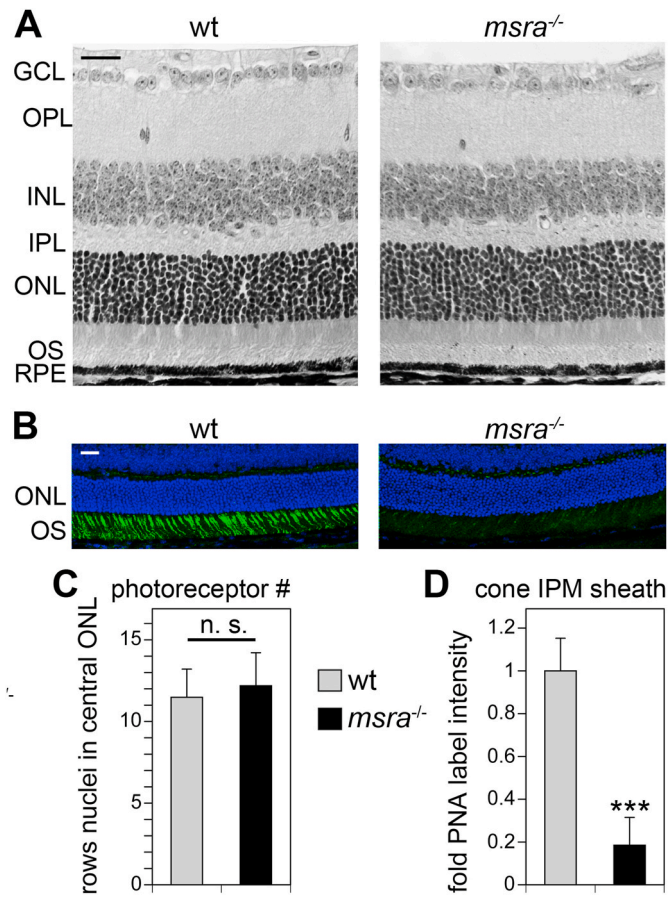

Fig. 3. $msra^{-/-}$ mice show normal gross retinal morphology but diminished PNA cone matrix labeling. Representative micrographs of retina cross sections obtained from 6-week old wt and $msra^{-/-}$ mice and stained with hematoxylin and eosin (**A**) or FITC-labeled PNA (green) and DAPI as nuclei counterstain (blue) (**B**). Scale bars, 50 μm. (**C**) Numbers of rows of photoreceptors in central retina were counted and are shown as mean ± s.e.m.; n = 3 mice. Student's *t*-test revealed no significant differences between strains (n. s.; $p > 0.05$). **(D)** Bar graphs show comparison of Image J quantification of PNA labeling intensity in images as shown in **B**, mean ± s.e.m.; n = 3 mice. Labeling intensity of wt retina was set as 1. Student's *t*-test revealed significant difference between wt and $msra^{-/-}$ PNA labeling intensity; ***$p < 0.001$. (For interpretation of the references to colour in this figure legend, the reader is referred to the Web version of this article.)

G,I, black bars), L/M-cone opsin (Fig. 5B, G,I, black bars), or S-cone opsin (Fig. 5C,G,I, black bars) in agreement with whole eye immunoblotting (Fig. 2). For rhodopsin, low magnification images confirmed that $msra^{-/-}$ rod outer segments have normal morphology and length throughout the retina (Fig. 5A, upper panels). Notably, high magnification images showed that cone arrestin labeling in $msra^{-/-}$ retina is attenuated (Fig. 5D). Indeed, cone arrestin steady-state level was decreased by 35% on average in 6 week-old $msra^{-/-}$ retina (Fig. 5D, G,I, black bars). PKC-α, a marker of rod bipolar cells, and calretinin, a protein expressed by several neurons of the inner retina but scarce in bipolar cells or photoreceptors [30] were indistinguishable in appearance and levels in wt and $msra^{-/-}$ retina (Fig. 5E,F,G,I, black bars). As before with light responses there was no difference in levels of marker proteins between 6 week-old and 6 month-old mice (Fig. 5, compare blot panels in G and H, and compare gray to black bars in I). Finally, TUNEL staining showed no evidence of apoptotic cell death in $msra^{-/-}$ retina (Supplemental Fig. S2). Altogether, these data demonstrate that MsrA deficiency mainly and specifically impacts cone photoreceptor functionality without provoking cone loss.

3.3. Cone photoreceptor function and matrix sheath are normal in dark-reared $msra^{-/-}$ mice

Dark rearing has been used by others to alleviate retinal dysfunction associated with oxidative stress (comprehensively reviewed in Ref. [31]). A recent study demonstrated benefit of dark rearing specifically for cone photoreceptors compromised by increased levels of retinal oxidative stress [32]. Here, we compared photoreceptor rod and cone functionality in wt and $msra^{-/-}$ mice born and raised in darkness up to 6 weeks of age. Scotopic ERGs revealed lower a-wave amplitudes in $msra^{-/-}$ mice (Fig. 6A, panel a-wave). This was surprising given we had not seen a significant difference in cyclic light-reared mice (Fig. 4). Direct comparison of ERGs recorded from dark-reared and cyclic light-reared mice (in experiments shown in Figs. 4 and 6, respectively) revealed that dark raising increased a-wave amplitudes of wt mice while it did not affect a-wave amplitudes of $msra^{-/-}$ mice (Supplemental Figs. S3A and B). Conversely, dark raising did not significantly change wt b-wave amplitudes but modestly increased $msra^{-/-}$ b-wave amplitudes (Supplemental Figs. S3C and D). We conclude that wt dark raising over prolonged periods of time renders wt rods slightly more sensitive to light, while, interestingly, this is not the case for $msra^{-/-}$ rods. Strikingly, dark-reared $msra^{-/-}$ mice did not differ in cone responses from dark-reared wt mice (Fig. 6B). Photopic average b-wave amplitudes of cyclic light- and dark-reared 6 week-old wt mice were identical at 100 μV and 106 μV, respectively (compare gray bars of Fig. 4D, bars 6 weeks, and Fig. 6B). In contrast, dark raising more than doubled the average photopic b-wave amplitude in $msra^{-/-}$ mice from 54 μV to 113 μV (compare black bars of Fig. 4D, bars 6 weeks, and Fig. 6B). Finally, PNA-labeled cone sheaths were as robust in dark-reared $msra^{-/-}$ mice as cone sheaths in dark-reared wt mice (Fig. 6C and D). We conclude from these intriguing findings that abnormalities in $msra^{-/-}$ mouse retina that are specific to cone photoreceptors are fully preventable.

4. Discussion

In this study, we explore how constitutive, global lack of MsrA in mice affects the functionality of RPE and neural retina *in vivo*. Our results establish $msra^{-/-}$ mice as a new experimental animal model in which robust and age-independent dysfunction specifically of photoreceptor cones can be prevented by dark rearing.

Acute manipulation of MsrA expression levels shows that MsrA in RPE cells in culture plays two distinct roles, protection from oxidative insult and support of mitochondrial respiration [27]. To first assess whether loss of MsrA *in vivo* increases oxidative stress, we examined protein oxidative modification in $msra^{-/-}$ tissues. Increased levels of protein carbonylation in whole eye extracts indicates increased oxidative stress in MsrA eyes in young adulthood, at 6 weeks of age. Both isolated neural retina and RPE/choroid show a trend toward increased protein oxidation as well that failed to reach statistical significance possibly due to sample to sample variability. For instance, isolated tissues have experienced slightly longer processing times during dissection as compared to whole eye collection.

Mitochondrial activity can be quantified specifically in live RPE by imaging membrane potential dependent fluorescent biosensor. Here, we found that $msra^{-/-}$ RPE cells *ex vivo* have significantly reduced mitochondrial activity matching our findings from acutely manipulated RPE cells in culture. Like in our earlier study, mitochondrial protein levels are normal in $msra^{-/-}$ eyes and enriched neural retina and RPE/choroid fractions. Moreover, decreased mitochondrial activity did not significantly alter ATP levels of RPE cells *in vivo*. This matches earlier findings demonstrating that RPE cells *in vivo* are capable of maintaining normal ATP levels even if mitochondrial respiration is abrogated [28]. We speculate that $msra^{-/-}$ RPE cells most likely compensate for reduced mitochondrial activity by adjusting glycolysis.

As $msra^{-/-}$ RPE *in situ* shares mitochondrial abnormality with RPE cells with acutely decreased MsrA that have phagocytic defects, we

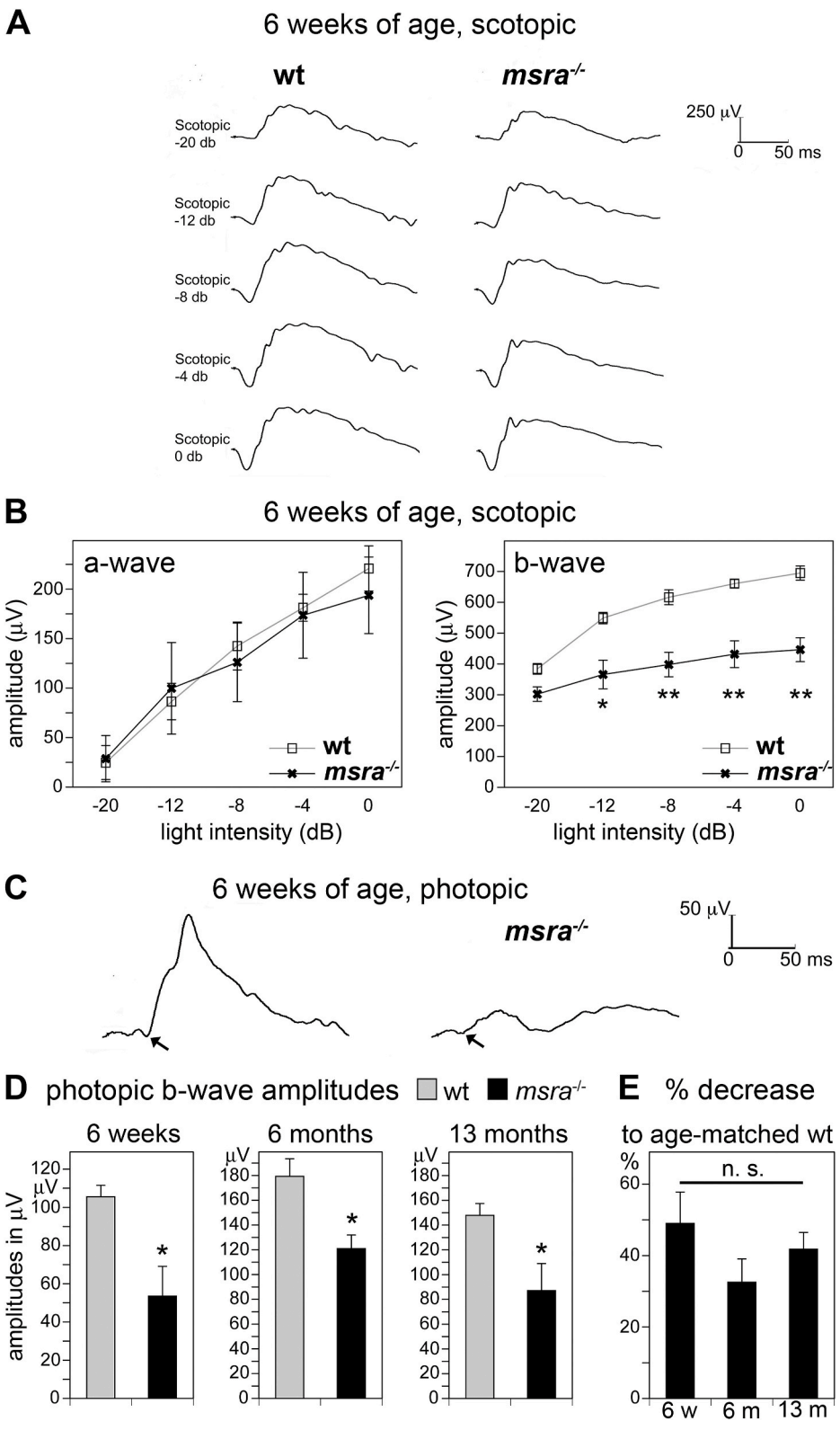

Fig. 4. ERG recordings reveal impaired light responses in adult *msra*$^{-/-}$ mice. Representative scotopic (**A**) and photopic (**C**) ERG recordings from 6-week-old wt and *msra*$^{-/-}$mice are shown. Arrows in **C** indicate photopic a-waves of wt and *msra*$^{-/-}$ mice, respectively. While photopic a-waves had obviously different appearance depending on genotype, they were not quantified given their small total size and possibly confounding issues of baseline stability, which might increase error. (**B**) Line graphs show response a- and b-wave amplitudes as indicated of scotopic ERGs; mean ± s.e.m.; n = 5 mice. Student's *t*-test revealed no significant differences between wt and *msra*$^{-/-}$ scotopic a-wave amplitudes indicative of rod photoreceptor function, but reduced b-wave amplitudes as indicated, $*p < 0.05$; $**p < 0.01$. (**D**) Bar graphs show photopic ERG b-wave amplitudes of the same cohorts that were tested in **B** (6 weeks; n = 5 each) and separate wt and *msra*$^{-/-}$ mouse cohorts (n = 4 each) tested at 6 and 13 months of age, respectively, as indicated. All bars show mean ± s.e.m.; Student's *t*-test revealed significant differences between wt and *msra*$^{-/-}$ photopic responses at all ages; $*p < 0.05$. (**E**) Comparison of the percentage of decrease of photopic b-wave amplitudes at the 3 ages tested in **D**, from data shown in **D**. Bars show average percent difference to wt of the same age (mean ± s.e.m.; n = 4–5). ANOVA showed that there was no significant difference in extent of decrease among ages; n. s.; $p > 0.05$.

tested whether *msra*$^{-/-}$ RPE is also impaired in its diurnal task of POS clearance phagocytosis. Indeed, we found that peak daily rod and cone POS phagosome content of *msra*$^{-/-}$ RPE *in situ* is significantly lower than in age- and strain-matched wt mice. We quantified POS phagosome content of the RPE at the time of the diurnal peak in wt RPE. It is possible that phagocytosis in *msra*$^{-/-}$ mice follows a different time course e.g. with a flattened peak but higher baseline POS uptake at other times over the 24-h period similar to mice lacking αvβ5 integrin [29]. Indeed, as seen in *itgb5*$^{-/-}$ mice, structural integrity and gross normal appearance of outer segments in *msra*$^{-/-}$ mice imply that rod and cone outer segment shedding are in balance with RPE phagocytosis avoiding accumulation of unengulfed POS or shortening of outer segments through excess phagocytosis. Unexpectedly, we found more severe effects of lack of MsrA on cone than on rod POS phagosome content. The

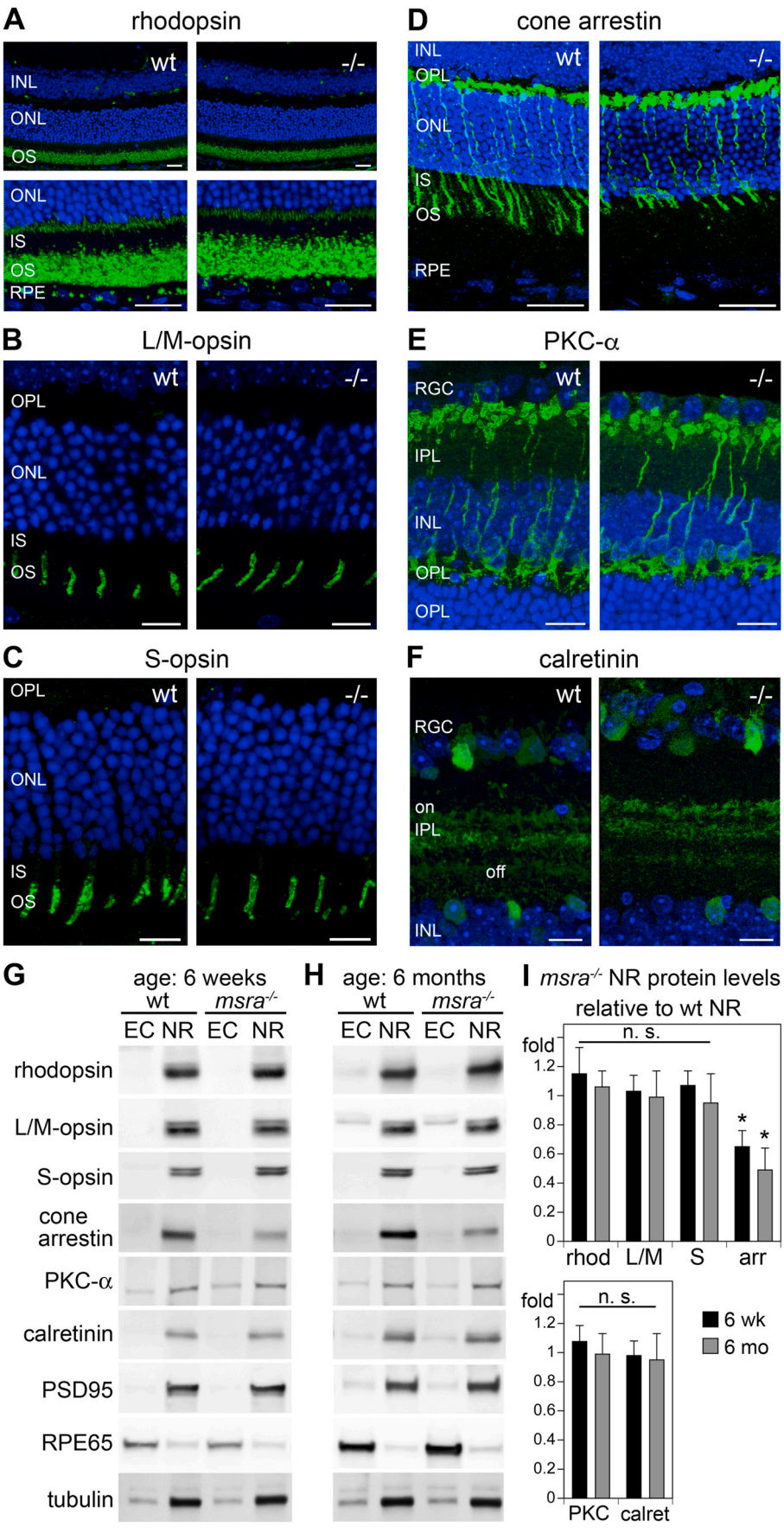

Fig. 5. Opsins and inner retinal marker proteins are similar to wt in *msra*$^{-/-}$ mice, but cone arrestin is decreased. **(A–F)** Retina cross sections obtained from 6-week old wt and *msra*$^{-/-}$ (−/−) mice were stained as indicated (green). Nuclei were counterstained with DAPI (blue). Rhodopsin labeling is shown at 2 magnifications (**A**). Fields were chosen to reveal cell type morphology. With respect to photoreceptors, we did not observe significant differences in labeling of photopigments rhodopsin (**A**), L/M − or S-cone opsin (**B**,**C**). However, cone arrestin staining was obviously attenuated in *msra*$^{-/-}$ retina (**D**). PKC-α marking rod bipolar cells and their arborization (**E**) and calretinin illustrating the ON and OFF *sublaminae* in the inner plexiform layer (**F**) were similar in wt and *msra*$^{-/-}$ retina. Scale bars, 25 μm. (**G-H**) Experiments show immunoblotting and quantification of marker proteins as indicated. Representative blots are shown of posterior eyecup (EC) and neural retina (NR) fractions of the same wt or *msra*$^{-/-}$ mouse at 6 weeks (**G**) or at 6 months of age (**H**). In addition to markers proteins also observed by microscopy, PSD95 and RPE65 served as tissue enrichment confirmation and load indicators for neural retina and RPE, respectively, and tubulin reprobing was used as additional indicator for sample load. (**I**) Quantification of blots as in **G** and **H** was performed to compare marker levels of wt and *msra*$^{-/-}$ tissues. Bars show average protein level of *msra*$^{-/-}$ neural retina at 6 weeks of age (black bars) and at 6 months of age (gray bars) compared to wt protein level at each age normalized for tubulin, which was set as 1 for each marker; mean ± s.e.m.; n = 3 mice of each genotype. Student's *t*-test showed that only reduction in cone arrestin was significant (*$p < 0.05$) and that extent of decrease did not differ between the 2 ages. (For interpretation of the references to colour in this figure legend, the reader is referred to the Web version of this article.)

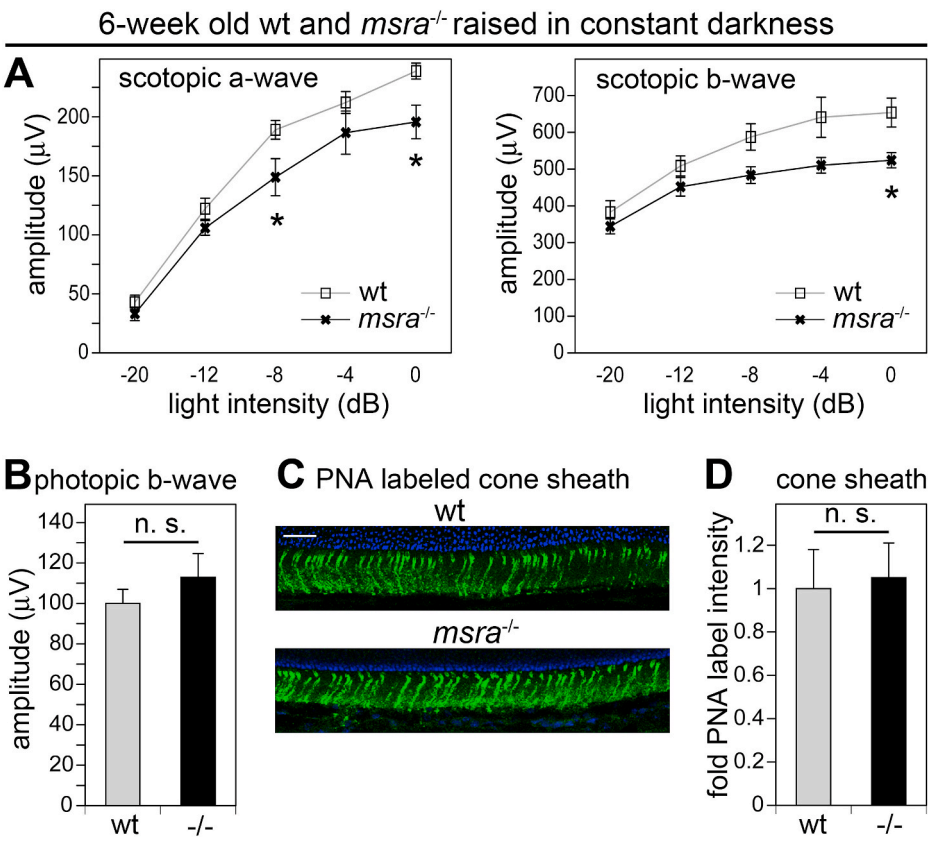

Fig. 6. Dark rearing of *msra*$^{-/-}$ mice does not restore rod-driven scotopic ERGS to wt levels but fully preserves cone-driven light responses in photopic ERGs and cone sheaths. Scotopic (**A**) and photopic (**B**) ERG assessment of 6-week-old wt and *msra*$^{-/-}$ mice born and reared in darkness, with ERG testing at 6 weeks of age and tissue harvest at 7 weeks of age; mean ± s.e.m.; n = 4 wt mice and 8 *msra*$^{-/-}$ mice. Note that wt but not *msra*$^{-/-}$ scotopic a-waves modestly increased with dark-rearing causing a significant difference of wt and *msra*$^{-/-}$ scotopic a-wave amplitudes at some flash intensities. Direct comparison of ERGs of dark- and cyclic light-reared mice is shown in Supplemental Fig. S3. Students' *t*-test revealed that the photopic b-wave of dark-reared *msra*$^{-/-}$ mice was identical to that of dark-reared wt mice (n. s.; $p > 0.05$). (**C**) Representative cone sheath fluorescence micrographs of tissue sections from dark-reared wt and *msra*$^{-/-}$ mice as indicated. Tissues were obtained 1 week after ERG testing. Scale bar, 50 µm. (**D**) Quantification of PNA labeling of images as in **C** showed no significant difference of wt and *msra*$^{-/-}$ cone sheaths if mice were dark-reared, mean ± s.e.m.; n = 3 mice of each genotype, n. s.; $p > 0.05$.

mechanism underlying this observation remains to be studied. If loss of MsrA was only affecting the RPE we might not expect a stronger effect on cone POS than on rod POS uptake unless the two processes were mechanistically distinct. We are not aware of evidence to date that RPE cells may employ a fundamentally different pathway for cone versus rod POS phagocytosis. However, this possibility cannot be discounted given that knowledge on cone POS phagocytosis remains scarce. Instead or in addition, impairment of photoreceptors themselves may also contribute to altered POS turnover with cones specifically affected. Identification of molecular pathways underlying either cone POS specific uptake by the RPE or photoreceptor-driven cone-POS turnover would be greatly facilitated by generation of cell type-specific MsrA null models and remain a task for future studies. We speculate that MsrA may support mitochondrial activity in cone photoreceptors like in RPE cells in culture [10]. In fact, a recent patch clamp study of single photoreceptors demonstrates that cones expend nearly twice as much energy as rods in darkness and that their ATP utilization in daylight remains high [33].

Our scotopic and photopic ERGs directly testing light responses by photoreceptor rods and cones further support a primary and specific abnormality of cones while rod light responses are normal. However, scotopic ERGs show modestly reduced b-wave amplitudes indicative of decreased activities of second order retinal neurons even at low intensity light stimulation, to which mainly rods respond. These results suggest that the retina in *msra*$^{-/-}$ mice may harbor modest inner retina abnormalities in addition to reduced input from impaired cones. Identifying these would be beyond the scope of our present study.

Focusing on the nature of cone dysfunction in *msra*$^{-/-}$ mice we found no evidence for age-dependent deterioration of cone light responses or any sign of apoptotic cell death or cell loss in *msra*$^{-/-}$ retina. Given normal rod function it is likely that rods in *msra*$^{-/-}$ retina can sustain cones via the rod-derived cone viability factor RdCVF [34,35]. Expression levels and appearance of S-cone and L/M-cone opsin photopigments are also indistinguishable between *msra*$^{-/-}$ and wt retina although cone arrestin is attenuated, a finding that is unexplained thus far. Future studies are needed to reveal why cones do not function normally in *msra*$^{-/-}$ mice. Grossly normal appearance, distribution and levels of cone opsins suggest that cones may form and remain viable in normal numbers in *msra*$^{-/-}$ retina. Nonetheless, it is possible that developmental abnormalities preclude cone cells from maturing fully. It is very intriguing -if also still rather enigmatic-that, PNA-lectin labeling of cone matrix sheaths is diminished in *msra*$^{-/-}$ retina. PNA specifically binds to galactosyl (β1-3) n-acetyl galactosamine residues [36]. As reported recently, PNA staining specifically labels proteoglycans IMPG1 and IMPG2 in the interphotoreceptor matrix [37]. These proteoglycans localize to both rod and cone matrices but terminal sialyl residues in rod sheaths may block PNA recognition resulting in PNA labeling specifically of cone matrix sheaths [38,39]. Loss of PNA labeling in *msra*$^{-/-}$ retina may thus be a result of either of lack of IMPG1 and IMPG2 or, more likely, of a conformational change precluding PNA recognition, for instance due to oxidative modification. While the precise nature of cone matrix sheath abnormality in *msra*$^{-/-}$ retina will require further studies, it is interesting to note that decreased MsrA levels in breast cancer tissue cause extracellular matrix degradation involving excess reactive oxygen species [40].

Our results show elevated oxidative burden in *msra*$^{-/-}$ eyes in mice as young as 6 weeks of age (the youngest age tested). Moreover, ERG testing does not support progressive worsening of cone dysfunction with aging. This is in contrast to many other mouse models of increased oxidative stress, which require long-term studies, for example see Ref. [29]. Photoreceptor cones in *msra*$^{-/-}$ retina are permanently inactive but do not degenerate. Moreover, our data show that the effects of MsrA loss on cone function and matrix can be fully prevented by dark rearing, a well-established retina-protective regimen [31,32,41]. Dark rearing is known to reduce the oxidative burden of the retina that stems from cyclic lighting at normal dim room light intensity levels [42,43]. However, dark rearing also alters specific retinal activities associated

with phototransduction and thus may affect retinal cells independently of oxidative effects [44,45]. Further studies will be needed to identify the mechanisms underlying the protective effect of dark rearing in *msra*$^{-/-}$ mice, and whether the effect is reversible or permanent. We suspect that dark rearing will prevent the excess protein carbonylation in *msra*$^{-/-}$ mice and expanded experiments are underway to test specifically when, how and via which molecular pathways environmental factors affect *msra*$^{-/-}$ cone dysfunction. Indeed, our study opens up new questions on how exactly loss of MsrA alters RPE and photoreceptor functionalities and serves as starting point for additional mechanistic experiments. Meanwhile, *msra*$^{-/-}$ mice will provide a practical and informative mouse model for studying photoreceptor cone physiology and interventions to support cone photoreceptors.

Data availability

Data that support the findings of this study are available from the corresponding author upon request.

Author contributions

FM and SCF designed the experiments. FM, YD, JAV, EFN, and SCF performed experiments and analyzed data. FM, JAV, and SCF wrote the manuscript. All authors reviewed and approved of the final manuscript.

Funding

This work was supported by the National Eye Institute of the National Institutes of Health grant number R01EY026215; SCF holds the Kim B. and Stephen E. Bepler Professorship in Biology.

Declaration of competing interest

The authors declare no conflict of interest with the research presented in the manuscript.

Acknowledgements

We than Dr. Nathan Brot (Florida Atlantic University) for sharing the *msra*$^{-/-}$ mouse strain. We thank Ms. Frances Kazal for excellent technical assistance.

Appendix A. Supplementary data

Supplementary data to this article can be found online at https://doi.org/10.1016/j.redox.2021.101918.

References

[1] Y. Nishimura, H. Hara, M. Kondo, S. Hong, T. Matsugi, Oxidative stress in retinal diseases, Oxid Med Cell Longev (2017) 4076518, 2017.
[2] J. Lu, A. Holmgren, The thioredoxin antioxidant system, Free Radic. Biol. Med. 66 (2014) 75–87.
[3] B.C. Lee, A. Dikiy, H.Y. Kim, V.N. Gladyshev, Functions and evolution of selenoprotein methionine sulfoxide reductases, Biochim. Biophys. Acta 1790 (2009) 1471–1477.
[4] J. Moskovitz, N.A. Jenkins, D.J. Gilbert, N.G. Copeland, F. Jursky, H. Weissbach, N. Brot, Chromosomal localization of the mammalian peptide-methionine sulfoxide reductase gene and its differential expression in various tissues, Proc. Natl. Acad. Sci. U. S. A. 93 (1996) 3205–3208.
[5] V.S. Sharov, D.A. Ferrington, T.C. Squier, C. Schöneich, Diastereoselective reduction of protein-bound methionine sulfoxide by methionine sulfoxide reductase, FEBS Lett. 455 (1999) 247–250.
[6] V.S. Sharov, C. Schöneich, Diastereoselective protein methionine oxidation by reactive oxygen species and diastereoselective repair by methionine sulfoxide reductase, Free Radic. Biol. Med. 29 (2000) 986–994.
[7] P.G. Sreekumar, R. Kannan, J. Yaung, C.K. Spee, S.J. Ryan, D.R. Hinton, Protection from oxidative stress by methionine sulfoxide reductases in RPE cells, Biochem. Biophys. Res. Commun. 334 (2005) 245–253.
[8] P.G. Sreekumar, D.R. Hinton, R. Kannan, Methionine sulfoxide reductase A: structure, function and role in ocular pathology, World J. Biol. Chem. 2 (2011) 184–192.
[9] J.W. Lee, N.V. Gordiyenko, M. Marchetti, N. Tserentsoodol, D. Sagher, S. Alam, H. Weissbach, M. Kantorow, I.R. Rodriguez, Gene structure, localization and role in oxidative stress of methionine sulfoxide reductase A (MSRA) in the monkey retina, Exp. Eye Res. 82 (2006) 816–827.
[10] Y. Dun, J. Vargas, N. Brot, S.C. Finnemann, Independent roles of methionine sulfoxide reductase A in mitochondrial ATP synthesis and as antioxidant in retinal pigment epithelial cells, Free Radic. Biol. Med. 65 (2013) 1340–1351.
[11] J. Moskovitz, S. Bar-Noy, W.M. Williams, J. Requena, B.S. Berlett, E.R. Stadtman, Methionine sulfoxide reductase (MsrA) is a regulator of antioxidant defense and lifespan in mammals, Proc. Natl. Acad. Sci. U. S. A. 98 (2001) 12920–12925.
[12] L.A. Brennan, W. Lee, T. Cowell, F. Giblin, M. Kantorow, Deletion of mouse MsrA results in HBO-induced cataract: MsrA repairs mitochondrial cytochrome c, Mol. Vis. 15 (2009) 985–999.
[13] R.L. Levine, Carbonyl modified proteins in cellular regulation, aging, and disease, Free Radic. Biol. Med. 32 (2002) 790–796.
[14] J. Moskovitz, D.B. Oien, Protein carbonyl and the methionine sulfoxide reductase system, Antioxidants Redox Signal. 12 (2010) 405–415.
[15] F. Mazzoni, T. Tombo, S.C. Finnemann, No difference between age-matched male and female C57BL/6J Mice in photopic and scotopic electroretinogram a- and b-wave amplitudes or in peak diurnal outer segment phagocytosis by the retinal pigment epithelium, Adv. Exp. Med. Biol. 1185 (2019) 507–511.
[16] S. Sethna, S.C. Finnemann, Analysis of rod outer segment phagocytosis by RPE cells in situ, Methods Mol. Biol. 935 (2013) 245–254.
[17] D.S. Lew, F. Mazzoni, S.C. Finnemann, Microglia inhibition delays retinal degeneration due to MerTK phagocytosis receptor deficiency, Front. Immunol. 11 (2020) 1463.
[18] G. Ying, K. Boldt, M. Ueffing, C.D. Gerstner, J.M. Frederick, W. Baehr, The small GTPase RAB28 is required for phagocytosis of cone outer segments by the murine retinal pigmented epithelium, J. Biol. Chem. 293 (2018) 17546–17558.
[19] C.C. Yu, E.F. Nandrot, Y. Dun, S.C. Finnemann, Dietary antioxidants prevent age-related retinal pigment epithelium actin damage and blindness in mice lacking αvβ5 integrin, Free Radic. Biol. Med. 52 (2012) 660–670.
[20] F. Mazzoni, C. Müller, J. DeAssis, D. Lew, W.M. Leevy, S.C. Finnemann, Non-invasive in vivo fluorescence imaging of apoptotic retinal photoreceptors, Sci. Rep. 9 (2019) 1590.
[21] E.K. Ahmed, C.R. Picot, A.L. Bulteau, B. Friguet, Protein oxidative modifications and replicative senescence of WI-38 human embryonic fibroblasts, Ann. N. Y. Acad. Sci. 1119 (2007) 88–96.
[22] F. Cabreiro, C.R. Picot, B. Friguet, I. Petropoulos, Methionine sulfoxide reductases: relevance to aging and protection against oxidative stress, Ann. N. Y. Acad. Sci. 1067 (2006) 37–44.
[23] I. Petropoulos, J. Mary, M. Perichon, B. Friguet, Rat peptide methionine sulphoxide reductase: cloning of the cDNA, and down-regulation of gene expression and enzyme activity during aging, Biochem. J. 355 (2001) 819–825.
[24] C.R. Picot, M. Perichon, J.C. Cintrat, B. Friguet, I. Petropoulos, The peptide methionine sulfoxide reductases, MsrA and MsrB (hCBS-1), are downregulated during replicative senescence of human WI-38 fibroblasts, FEBS Lett. 558 (2004) 74–78.
[25] H. Buss, T.P. Chan, K.B. Sluis, N.M. Domigan, C.C. Winterbourn, Protein carbonyl measurement by a sensitive ELISA method, Free Radic. Biol. Med. 23 (1997) 361–366.
[26] L. Lu, S.F. Hackett, A. Mincey, H. Lai, P.A. Campochiaro, Effects of different types of oxidative stress in RPE cells, J. Cell. Physiol. 206 (2006) 119–125.
[27] Y. Dun, J. Vargas, N. Brot, S.C. Finnemann, Independent roles of methionine sulfoxide reductase A in mitochondrial ATP synthesis and as antioxidant in retinal pigment epithelial cells, Free Radic. Biol. Med. 65 (2013) 1340–1351.
[28] C. Zhao, D. Yasumura, X. Li, M. Matthes, M. Lloyd, G. Nielsen, K. Ahern, M. Snyder, D. Bok, J.L. Dunaief, M.M. LaVail, D. Vollrath, mTOR-mediated dedifferentiation of the retinal pigment epithelium initiates photoreceptor degeneration in mice, J. Clin. Invest. 121 (2011) 369–383.
[29] E.F. Nandrot, Y. Kim, S.E. Brodie, X. Huang, D. Sheppard, S.C. Finnemann, Loss of synchronized retinal phagocytosis and age-related blindness in mice lacking αvβ5 integrin, J. Exp. Med. 200 (2004) 1539–1545.
[30] B. Pasteels, J. Rogers, F. Blachiel, R. Pochet, Calbindin and calretinin localization in retina from different species, Vis. Neurosci. 5 (2009) 1–16.
[31] D.M. Paskowitz, M.M. LaVail, J.L. Duncan, Light and inherited retinal degeneration, Br. J. Ophthalmol. 90 (2006) 1060–1066.
[32] A. Trouillet, E. Dubus, J. Degardin, A. Estivalet, I. Ivkovic, D. Godefroy, D. Garcia-Ayuso, M. Simonutti, I. Sahly, J.A. Sahel, A. El-Amraoui, C. Petit, S. Picaud, Cone degeneration is triggered by the absence of USH1 proteins but prevented by antioxidant treatments, Sci. Rep. 8 (2018) 1968.
[33] N.T. Ingram, G.L. Fain, A.P. Sampath, Elevated energy requirement of cone photoreceptors, Proc. Natl. Acad. Sci. Unit. States Am. 117 (2020) 19599.
[34] N. Aït-Ali, R. Fridlich, G. Millet-Puel, E. Clérin, F. Delalande, C. Jaillard, F. Blond, J. Perrocheau, S. Reichman, L.C. Byrne, A. Olivier-Bandini, J. Bellalou, E. Moyse, F. Bouillaud, X. Nicol, D. Dalkara, vA. an Dorsselaer, J.A. Sahel, T. Léveillard, Rod-derived cone viability factor promotes cone survival by stimulating aerobic glycolysis, Cell 161 (2015) 817–832.
[35] T. Léveillard, J.A. Sahel, Rod-derived cone viability factor for treating blinding diseases: from clinic to redox signaling, Sci. Transl. Med. 2 (2010) 26ps16.
[36] R.D. Cummings, M.E. Etzler, Antibodies and lectins in glycan analysis, in: A. Varki, R.D. Cummings, J.D. Esko, H.H. Freeze, P. Stanley, C.R. Bertozzi, G.W. Hart, M.

E. Etzler (Eds.), Essentials of Glycobiology, Cold Spring Harbor Laboratory Press, © Cold Spring Harbor, (NY), 2009.
[37] E.M. Salido, V. Ramamurthy, Proteoglycan IMPG2 shapes the interphotoreceptor matrix and modulates vision, J. Neurosci. 40 (2020) 4059–4072.
[38] F. Uehara, D. Yasumura, M.M. LaVail, Rod and cone-associated interphotoreceptor matrix in the rat retina, Invest. Ophthalmol. Vis. Sci. 32 (1991) 285–292.
[39] F. Uehara, M. Ozawa, M. Sameshima, K. Unoki, A. Okubo, T. Yanagita, M. Sugata, N. Iwakiri, Y. Maeda, T. Muramatsu, et al., Differential expression of mRNA for alpha 2,3-sialyltransferase during development of rat retina, Jpn. J. Ophthalmol. 39 (1995) 248–253.
[40] A. De Luca, F. Sanna, M. Sallese, C. Ruggiero, M. Grossi, P. Sacchetta, C. Rossi, V. De Laurenzi, C. Di Ilio, B. Favaloro, Methionine sulfoxide reductase A down-regulation in human breast cancer cells results in a more aggressive phenotype, Proc. Natl. Acad. Sci. U. S. A. 107 (2010) 18628–18633.
[41] T. Cronin, A. Lyubarsky, J. Bennett, Dark-rearing the rd10 mouse: implications for therapy, Adv. Exp. Med. Biol. 723 (2012) 129–136.
[42] D.T. Organisciak, R.M. Darrow, L. Barsalou, R.A. Darrow, R.K. Kutty, G. Kutty, B. Wiggert, Light history and age-related changes in retinal light damage, Invest. Ophthalmol. Vis. Sci. 39 (1998) 1107–1116.
[43] D.T. Organisciak, R.M. Darrow, L. Barsalou, R.K. Kutty, B. Wiggert, Susceptibility to retinal light damage in transgenic rats with rhodopsin mutations, Invest. Ophthalmol. Vis. Sci. 44 (2003) 486–492.
[44] B.A. Berkowitz, R.H. Podolsky, A.M. Berri, K. Dernay, E. Graffice, F. Shafie-Khorassani, R. Roberts, Dark rearing does not prevent rod oxidative stress in vivo in Pde6brd10 mice, Invest. Ophthalmol. Vis. Sci. 59 (2018) 1659–1665.
[45] B.A. Berkowitz, R.H. Podolsky, K.L. Childers, S.L. Roche, T.G. Cotter, E. Graffice, L. Harp, K. Sinan, A.M. Berri, M. Schneider, H. Qian, S. Gao, R. Roberts, Rod photoreceptor neuroprotection in dark-reared Pde6brd10 mice, Invest. Ophthalmol. Vis. Sci. 61 (2020) 14.